

Two-dimensional van der Waals p - n junction of InSe/phosphoreneJ. E. Padilha,^{1,*} R. H. Miwa,^{2,†} Antonio J. R. da Silva,^{3,‡} and A. Fazzio^{4,§}¹*Campus Avançado Jandaia do Sul, Universidade Federal do Paraná, Jandaia do Sul, PR, Brazil*²*Instituto de Física, Universidade Federal de Uberlândia, Caixa Postal 593, 38400-902, Uberlândia, MG, Brazil*³*Instituto de Física, Universidade de São Paulo, CP 66318, 05315-970, São Paulo, SP, Brazil
and Laboratório Nacional de Luz Síncrotron, CP 6192, 13083-970, Campinas, SP, Brazil*⁴*Brazilian Nanotechnology National Laboratory(LNNano)/CNPEM, 130830-979, Campinas, SP, Brazil
(Received 10 February 2017; revised manuscript received 4 April 2017; published 19 May 2017)*

We investigate the energetic stability and the structural and electronic properties of semiconductor/semiconductor and semiconductor/metal 2D van der Waals heterostructures composed by combinations of single layer InSe, bilayer phosphorene (BP), and graphene. For the semiconductor/semiconductor BP/InSe heterostructure, we found that the lowest (highest) unoccupied (occupied) states lie on the InSe (BP) layers, giving rise to a type-II band alignment, with electrons (holes) localized in the InSe (BP) layers. The semiconductor/metal interface composed by a single layer of InSe stacked on graphene (InSe/G) presents a n -type Schottky barrier, which can be tuned by applying an external electric field perpendicular to the InSe/G interface (E_{\perp}^{ext}). Upon further increase of E_{\perp}^{ext} , the InSe/G contact becomes Ohmic, promoting a net charge transfer from the graphene sheet to the InSe layer, n -type doping. This is in contrast with the other semiconductor/metal van der Waals heterojunction, BP/G, where the BP sheet becomes p -type doped as a function of E_{\perp}^{ext} . Exploiting the electron-hole separation in BP/InSe, and the formation of Ohmic contacts at the InSe/G and BP/G interfaces, we propose a p - n junction composed by p -type BP and n -type InSe, with the graphene acting as electrodes and also as a source of electrons/holes in InSe/BP.

DOI: [10.1103/PhysRevB.95.195143](https://doi.org/10.1103/PhysRevB.95.195143)**I. INTRODUCTION**

The synthesis of new materials by stacking atomic layers with different electronic properties, as the epitaxial growth of semiconductor superlattices [1], has been the subject of intense studies for several decades, most of them working the development of new electronic devices as well as the fundamental research [2]. A few years ago, the concept of van der Waals (vdW) heterostructures was introduced by Geim and Grigorieva [3]. Such vdW heterostructures are synthesized by stacking two dimensional (2D) crystalline atomic layers, with no chemical bonds between them. In this case, the formation of sharp interfaces is not constrained by the lattice mismatch between the stacked layers, and thus we may have a huge variety of vdW heterostructures based on different combinations of 2D materials. Within this scenario, we can infer that given a set of desired physical/chemical properties, vdW heterostructures, can be designed based on a suitable choice of the 2D compounds. Here, in order to make a successful 2D material engineering, the understanding of the electronic and structural properties of the interfaces between those 2D compounds plays a fundamental role.

van der Waals heterostructures composed by metal chalcogenides, for instance, GaSe [4], In₂Se₃ [5,6], and InSe [7–12], have recently been used as key elements for optoelectronic

and nanoelectronic applications [4,13–16]. Those materials are characterized by high on-off current ratio ($\sim 10^3$), high electron mobility [10^3 cm²/(V s)] [4,14,15], and large broadband spectral response [17]. In addition, they are mechanically flexible [17] and, similar to the transition metal dichalcogenides, their band gap can be tuned by the number of layers, as well as through an external electrical field [8,14,18,19]. Focusing on the 2D electronic devices, very recently Lee *et al.* synthesized a 2D p - n junction by stacking MoS₂ and WSe₂ layers [20]. However, there are several issues to be addressed in order to use those 2D vdW heterostructures for device application [3,21,22]. For instance, the contact between the active region and the electrodes as discussed in Ref. [23].

Graphene has been used to build up semiconductor/metal junctions based on 2D systems [24–27]. Similar to its 3D counterpart, the characterization of the Schottky barrier at the semiconductor/metal interface is quite important to the electronic properties of 2D systems. For instance, the height of the Schottky barrier as a function of an external electric (gate) field. Indeed, the control of the Schottky barrier and the p -type doping of a 2D vdW heterostructure composed by a bilayer phosphorene on graphene (BP/G) have been studied through *ab initio* density functional calculations [28]. As we have testified for three dimensional heterostructures and superlattices, computational simulations (based on atomistic approaches) play a quite important role on the study of the electronic and structural properties, and provide helpful information in order to design semiconductor/semiconductor and semiconductor/metal 2D vdW heterojunctions.

In this work, based on first-principles calculations, we investigate the electronic and the structural properties of 2D semiconductor/semiconductor and semiconductor/metal vdW heterojunctions. For the former, we find that the bilayer

*jose.padilha@ufpr.br

†hiroki@ufu.br

‡jose.roque@lnls.br

§fazzio@if.usp.br; also at Centro de Ciências Naturais e Humanas, Universidade Federal do ABC, Santo André, São Paulo, 09210-170, Brazil.

phosphorene lying on a single layer InSe (BP/InSe) presents a type-II band alignment, with the holes/electrons localized in the BP/InSe layers. Meanwhile, single layer InSe on graphene (InSe/G) characterizes a 2D semiconductor/metal vdW heterojunction. We show that InSe/G presents a n -type Schottky barrier, being in contrast with the p -type Schottky barrier verified in BP/G [28]. Furthermore, both Schottky barriers can be tuned upon an external electric field normal to the InSe/G and BP/G interfaces (E_{\perp}^{ext}), where semiconductor/metal heterojunctions become Ohmic for E_{\perp}^{ext} larger than ~ 2 V/nm (for both systems) in absolute values. Finally, based upon our findings for the semiconductor/semiconductor (BP/InSe) and semiconductor/metal (InSe/G and BP/G) vdW interfaces, we propose a p - n vdW heterojunction, with the graphene sheet acting as a contact and source of electrons/holes in the n -type/ p -type InSe/BP interface.

II. METHODS

The structural and electronic properties of the 2D van der Waals heterostructures were investigated by the state-of-the-art *ab initio* simulations, based on the density functional theory (DFT) as implemented in the VASP code [29,30]. We use the generalized gradient approximation for the exchange and correlation potential, as proposed by Perdew-Burk-Ernzerhof (PBE) [31], together with the projector augmented wave potential (PAW) [32,33] to treat the ion-electron interactions, and a plane-wave cutoff energy of 500 eV. To correctly describe the effect of a van der Waals interaction, we employed a dispersion-corrected DFT method (optB88-vdW) [34,35], which has been demonstrated to be a reliable approach to describe dispersive forces in 2D systems [36]. With the optimized structures, the HSE06 hybrid functional [37,38] was used to calculate the band structures of the systems. In general, HSE06 hybrid functional provides more accurate values of band gaps, fixing the underestimated values obtained by using the standard DFT-PBE approach [39], as well as ionization potential, electronic affinity, and work function in good agreement with the experimental measurements. The band structures, work functions, and band edges were aligned with respect to the vacuum level, obtained via the electrostatic potentials of the systems.

III. RESULTS AND DISCUSSION

Initially we examine the energetic stability, and the electronic properties of a 2D semiconductor van der Waals heterostructure composed by a bilayer phosphorene on top of a single layer InSe (BP/InSe) [Fig. 1(a)]. The BP/InSe supercell is defined by the lattice vectors \mathbf{c}_1 and \mathbf{c}_2 indicated by the dotted square in Fig. 1(a). Here, in order to minimize the lattice mismatch between the BP and the InSe layers, due to the periodic boundary conditions, we have considered surface periodicities of (2×2) and (1×2) for the BP and InSe, respectively, where the InSe (BP) sheet is strained by 3.5% (-3.21%) in the x direction and compressed by -3.21% (8.55%) in the y direction. All the atomic positions and lattice vectors of BP/InSe were fully relaxed; we found a vertical (interlayer) distance of 3.26 \AA [$d_{\text{BP/InSe}}$ in Fig. 1(a)]. Such a vertical distance is larger than the sum of the covalent radii

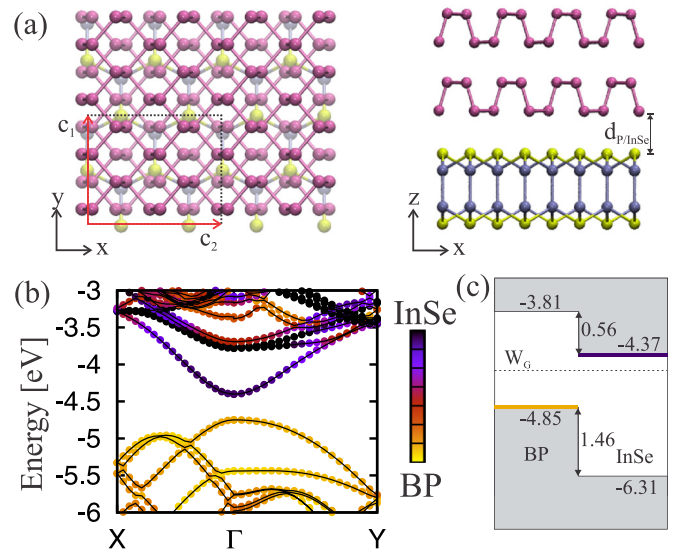


FIG. 1. (a) Top view (left panel) and side view (right panel) of a bilayer phosphorene on top of a single layer InSe. The supercell used in the calculations is defined by the vectors \mathbf{c}_1 and \mathbf{c}_2 , using the symmetry of the bilayer phosphorene unit cell. (b) Projected band structure of the bilayer phosphorene on single layer InSe. The lighter (yellow) projection comes from the bilayer phosphorene and the darker (black) comes from the InSe layer. (c) Schematic representation of the band edges of the heterostructure. All alignments were made with respect to the vacuum level.

of the P and In/Se atoms, with no chemical bonds at the BP/InSe interface region. The energetic stability of BP/InSe was examined by comparing the total energies of the final BP/InSe system ($E_{\text{BP/InSe}}$), with ones of the isolated components (E_{BP} and E_{InSe}), $E_{\text{BP/InSe}}^b = E_{\text{BP}} + E_{\text{InSe}} - E_{\text{BP/InSe}}$. The latter terms, E_{BP} and E_{InSe} , were obtained by considering the strained (2×2) and (1×2) supercells, respectively. We found that the formation of BP/InSe interface is an exothermic process, $E_{\text{BP/InSe}}^b = 9.03 \text{ meV/\AA}^2$. Those findings of $E_{\text{BP/InSe}}^b$ and equilibrium vertical distance $d_{\text{BP/InSe}}$ indicate that the energetic stability of the BP/InSe interface is mediated by vdW interactions.

The electronic states of the BP and the InSe layers are weakly perturbed upon the formation of BP/InSe; for instance, we found that the energy position of the valence band maximum (VBM) and the conduction band minimum (CBM) of BP and InSe change by less than 0.05 eV. Figure 1(b) shows the electronic band structure of BP/InSe projected on the BP and InSe layers. BP/InSe presents a semiconducting character, with a direct energy gap of 0.48 eV at the Γ point. The energies in Fig. 1(b) are presented with respect to the vacuum level, where VBM lies on the BP layer while the CBM is localized in InSe. The BP/InSe heterojunction presents a type-II band alignment, as depicted in Fig. 1(c), with a valence/conduction band offset of 1.46/0.56 eV [41], which is suitable in order to promote the electron-hole separation. In this case, we have electrons localized in the InSe layer, and holes in the BP layer. In addition, it is worth noting that the work function of the free standing graphene sheet, -4.5 eV [W_G in Fig. 1(c)], lies between the VBM of BP and the CBM of InSe. Such an alignment of the energy

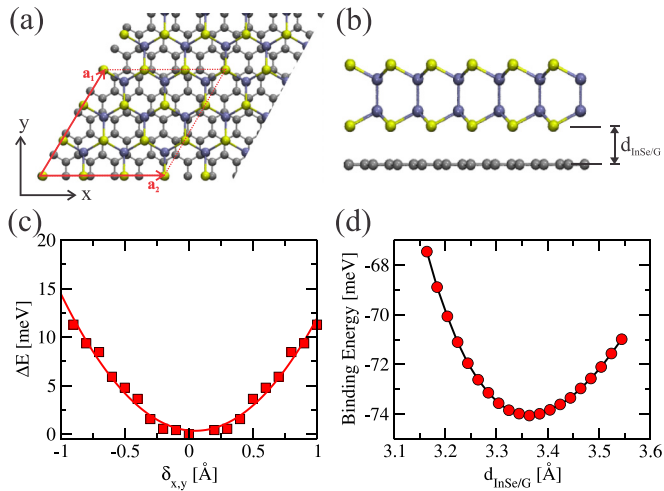


FIG. 2. (a) Top view of a single layer InSe on top of graphene showing the supercell used in the calculations (dashed region) defined by the vectors \mathbf{a}_1 and \mathbf{a}_2 . (b) Side view of a single layer InSe on top of graphene showing the interlayer distance $d_{\text{InSe/G}}$. (c) Evolution of the total energy difference as function of displacements $\delta_{x/y}$ of the InSe layer relative to graphene, taking the origin at the lowest energy configuration. (d) Binding energy as function of the distance $d_{\text{InSe/G}}$. The binding energy was defined per graphene unit cell.

levels of BP and InSe can be exploited in order to control the electronic charge transfers and the Schottky barrier at the semiconductor/metal (i.e., BP/G and InSe/G) interface. Indeed, 2D heterostructures composed by bilayer-phosphorene and graphene (BP/G) present a p -type Schottky barrier, which can be tuned by an external electric field perpendicular to the BP/G interface (E_{\perp}^{ext}) [28]. In contrast, vdW heterostructures composed by a graphene sheet on the InSe layer (InSe/G) may present a n -type Schottky barrier (Φ^{B}), also tunable by an external electric field, E_{\perp}^{ext} .

In Figs 2(a) and 2(b) we present the top and side views of InSe/G. Both systems exhibit a hexagonal lattice, with lattice vectors of 4.09 Å (InSe) and 2.46 Å (graphene). In order to minimize the strain induced by the lattice mismatch between InSe and graphene, we have considered supercells with (3×3) and (5×5) periodicities for InSe and graphene, respectively. In this case, the lattice mismatch reduces to 0.24 %. Similar to what we have done for the BP/InSe heterostructure, all the atomic positions of InSe/G were fully relaxed, and the energetically most stable configuration was obtained by considering lateral displacements of the InSe

monolayer along the x and y directions ($\delta_{x/y}$). Our total energy results, presented in Fig. 2(c), allow us to infer that the increase of the total energy, ΔE , is isotropic with respect to the atomic displacements parallel to the InSe/G interface. For the lowest energy configuration, we determined the binding energy between the InSe layer and graphene, where we found $E_{\text{InSe/G}}^b$ of 74 meV per (1×1) graphene unit cell ($6.90 \text{ meV}/\text{\AA}^2$), which is close to the ones for other van der Waals systems, such as graphite ($\sim 60 \text{ meV}$), h-BN (65 meV), and graphene/phosphorene heterostructure (60 meV) [28,42]. In Fig. 2(d) we present the binding energy of InSe/G as a function of the vertical distance ($d_{\text{InSe/G}}$) between the InSe monolayer and the graphene sheet. At the equilibrium geometry we found $d_{\text{InSe/G}}$ of 3.36 Å, suggesting the absence of chemical bonds at the InSe/G interface, and thus supporting the vdW interaction between the InSe and graphene monolayers.

Although there is a charge density rearrangement at the InSe/G interface, the energy bands of the isolated systems are weakly perturbed upon the formation of the InSe/G system. In Fig. 3 we present the energy bands of InSe/G, including the projection of the electronic states on the InSe monolayer [Fig. 3(a)] and graphene sheet [Fig. 3(b)]. We find that (i) the energy positions of the VBM and CBM of the InSe monolayer are perturbed by less than 0.06 eV, when compared with the ones of pristine InSe, and (ii) the Dirac cone structure of graphene is slightly perturbed due to the formation of the InSe/G interface. For instance, the work function of graphene ($W_{\text{G}} = -4.51 \text{ eV}$) reduces by 0.03 eV in InSe/G, $W_{\text{InSe/G}} = -4.54 \text{ eV}$ [Fig. 3(c)]. Since the interaction between the InSe and the graphene layers is ruled by vdW forces, with no chemical bonds between the metal and the semiconductor, the Schottky barrier height can be estimated by using the Schottky-Mott approach [43], namely $\Phi^{\text{B}} = E_{\text{InSe}}^{\text{CBM}} - W_{\text{InSe/G}} = 0.21 \text{ eV}$, which is indicated as Δ_{CB} in Fig. 4(a).

Turning on an external electric field perpendicular to the InSe/G interface, E_{\perp}^{ext} , we can control the Schottky barrier height in 2D vdW heterostructures [28]. E_{\perp}^{ext} gives rise to a potential gradient normal to the InSe/G interface, promoting the control of the energy positions of the CBM and VBM of the semiconductor (InSe) with respect to the Fermi level of the metal (G), indicated as Δ_{CB} and Δ_{VB} in Fig. 4(a). As depicted in Fig. 4(b) [Fig. 4(c)], the energy bands of InSe move downward (upward) with respect to the Dirac point for a positive (negative) electric field of $E_{\perp}^{\text{ext}} = 2.5 \text{ V/nm}$ (-2.5 V/nm). The evolution of Δ_{CB} and Δ_{VB} , as a function of the external electric field, is summarized in Fig. 4(d), showing that we can continuously tune the Schottky barrier height. We

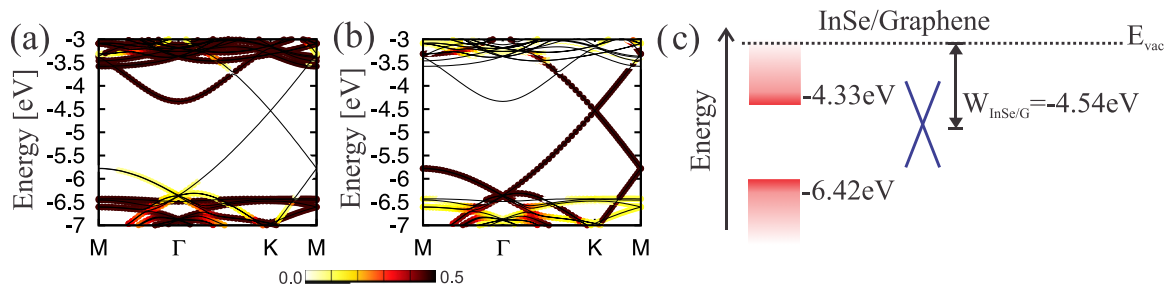


FIG. 3. Projected band structure of the 2D heterostructure of InSe/G in the (a) InSe layer and (b) graphene layer. (c) Band edges of the composed heterostructure aligned with respect to the vacuum level. The solid black lines stand for the total band structure.

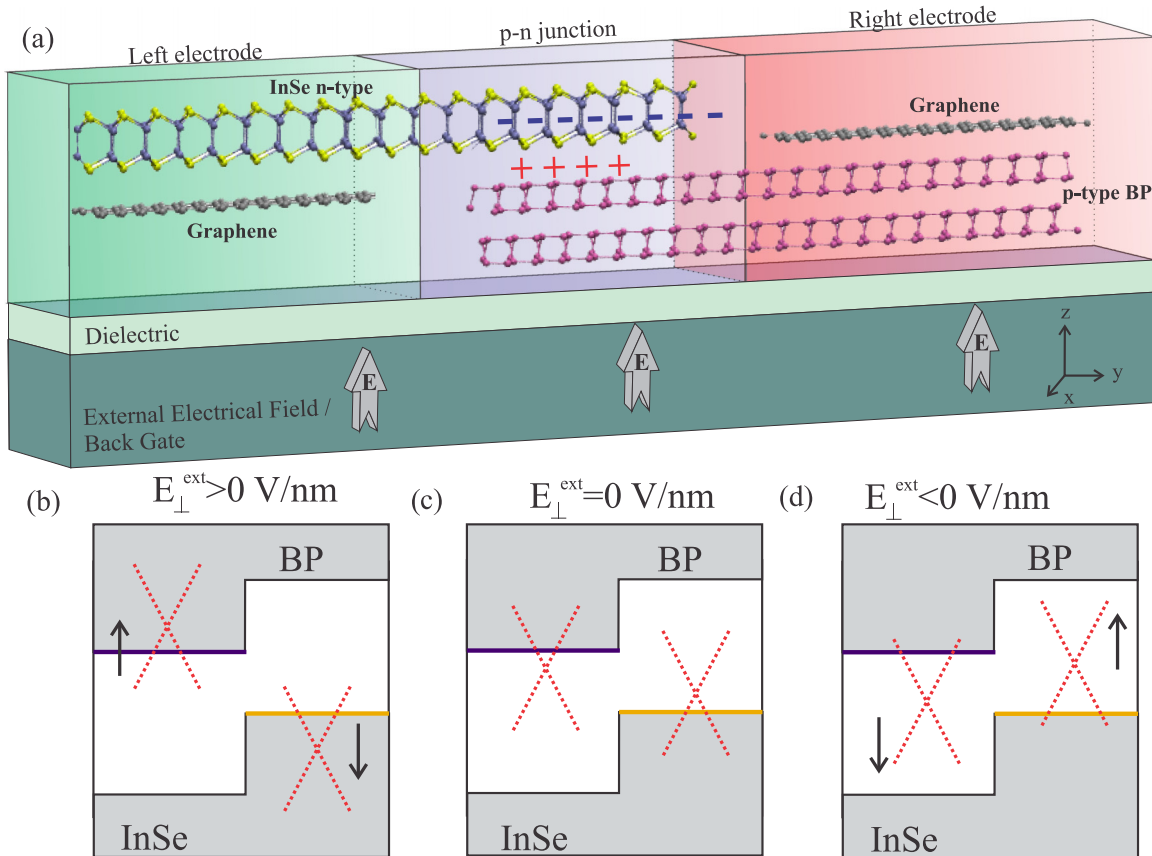


FIG. 6. (a) Schematic representation of the p - n junction based on a graphene/InSe/bilayer phosphorene van der Waals heterostructure. The left and right electrodes are composed with InSe/graphene and bilayer phosphorene/graphene and the p - n region consists of InSe/bilayer phosphorene. Representation of the position of the band edges and position of the Dirac cone for (a) $E_{\perp}^{\text{ext}} > 0$ V/nm, (b) $E_{\perp}^{\text{ext}} = 0$ V/nm, and (c) $E_{\perp}^{\text{ext}} < 0$ V/nm. The arrows represent the direction of the Dirac cone movement due to the applied electric field.

other hand, in the present study, we find that InSe/G presents a n -type Schottky barrier, and the InSe/G interface becomes Ohmic for $E_{\perp, G \rightarrow \text{InSe}}^{\text{ext}}$ larger than 1.5 V/nm. Based upon those findings, we propose a 2D vdW p - n heterojunction composed by bilayer-phosphorene stacked on a single layer InSe, BP/InSe, where the p -type (n -type) doping levels of the BP (InSe) layers can be tuned by an external electric field, E_{\perp}^{ext} , at the semiconductor/metal (BP/G and InSe/G) contact regions.

ACKNOWLEDGMENTS

This work was supported by the Brazilian agencies FAPESP, FAPEMIG, and CNPq. We would like to acknowledge computing time provided on the Blue Gene/Q supercomputer supported by the Research Computing Support Group (Rice University) and Laboratório de Computação Científica Avançada (Universidade de São Paulo).

- [1] L. Ezaki and R. Tsu, *IBM J. Res. Dev.* **14**, 61 (1970).
- [2] L. P. Kouwenhoven, A. T. Johnson, N. C. van der Vaart, C. J. P. M. Harmans, and C. T. Foxon, *Phys. Rev. Lett.* **67**, 1626 (1991).
- [3] A. K. Geim and I. V. Grigorieva, *Nature (London)* **499**, 419 (2013).
- [4] S. Lei, L. Ge, Z. Liu, S. Najmaei, G. Shi, G. You, J. Lou, R. Vajtai, and P. M. Ajayan, *Nano Lett.* **13**, 2777 (2013).
- [5] J. O. Island, S. I. Blanter, M. Buscema, H. S. J. van der Zant, and A. Castellanos-Gomez, *Nano Lett.* **15**, 7853 (2015).
- [6] J. Zhou, Q. Zeng, D. Lv, L. Sun, L. Niu, W. Fu, F. Liu, Z. Shen, C. Jin, and Z. Liu, *Nano Lett.* **15**, 6400 (2015).
- [7] Y. Zhou, B. Deng, Y. Zhou, X. Re, J. Yin, C. Jin, Z. Liu, and H. Peng, *Nano Lett.* **16**, 2103 (2016).
- [8] L. Debbichi, O. Eriksson, and S. Lebègue, *J. Phys. Chem. Lett.* **6**, 3098 (2015).
- [9] S. Lei, X. Wang, B. Li, J. Kang, Y. He, A. George, L. Ge, Y. Gong, P. Dong, Z. Jin, G. Brunetto, W. Chen, Z.-T. Lin, R. Baines, D. S. Galvão, J. Lou, E. Barrera, K. Banerjee, R. Vajtai, and P. Ajayan, *Nat. Nanotechnol.* **11**, 465 (2016).
- [10] G. W. Mudd, S. A. Svatek, L. Hague, O. Makarovskiy, Z. R. Kudrynskiy, C. J. Mellor, P. H. Beton, L. Eaves, K. S. Novoselov, Z. D. Kovalyuk, E. E. Vdovin, A. J. Marsden, N. R. Wilson, and A. Patanè, *Adv. Mater.* **27**, 3760 (2015).
- [11] S. A. Svatek, G. W. Mudd, Z. R. Kudrynskiy, O. Makarovskiy, Z. D. Kovalyuk, C. J. Mellor, L. Eaves, P. H. Beton, and A. Patanè, *J. Phys.: Conf. Ser.* **647**, 012001 (2015).

- [12] W. Luo, Y. Cao, P. Hu, K. Cai, Q. Feng, F. Yan, T. Yan, X. Zhang, and K. Wang, *Adv. Opt. Mater.* **3**, 1418 (2015).
- [13] S. Lei, F. Wen, L. Ge, S. Najmaei, A. George, Y. Gong, W. Gao, Z. Jin, B. Li, J. Lou, J. Kono, R. Vajtai, P. Ajayan, and N. J. Halas, *Nano Lett.* **15**, 3048 (2015).
- [14] W. Feng, W. Zheng, X. S. Chen, G. Liu, and P. A. Hu, *ACS Appl. Mater. Interfaces* **7**, 26691 (2015).
- [15] S. Sucharitakul, N. J. Goble, U. R. Kumar, R. Sankar, Z. A. Bogorad, F.-C. Chou, Y.-T. Chen, and X. P. A. Gao, *Nano Lett.* **15**, 3815 (2015).
- [16] S. Lei, F. Wen, B. Li, Q. Wang, Y. Huang, Y. Gong, Y. He, P. Dong, J. Bellah, A. George, L. Ge, J. Lou, N. J. Halas, R. Vajtai, and P. M. Ajayan, *Nano Lett.* **15**, 259 (2015).
- [17] S. R. Tamalampudi, Y.-Y. Lu, U. R. Kumar, R. Sankar, C.-D. Liao, B. K. Moorthy, C.-H. Cheng, F. C. Chou, and Y.-T. Chen, *Nano Lett.* **14**, 2800 (2014).
- [18] J. E. Padilha, H. Peelaers, A. Janotti, and C. G. Van de Walle, *Phys. Rev. B* **90**, 205420 (2014).
- [19] S. Lei, L. Ge, S. Najmaei, A. George, R. Kappera, J. Lou, M. Chhowalla, H. Yamaguchi, G. Gupta, R. Vajtai, A. D. Mohite, and P. M. Ajayan, *ACS Nano* **8**, 1263 (2014).
- [20] C.-H. Lee, G.-H. Lee, A. M. van der Zande, W. Chen, Y. Li, M. Han, X. Cui, G. Arefe, C. Nuckolls, T. F. Heinz, J. Guo, J. Hone, and P. Kim, *Nat. Nanotechnol.* **9**, 676 (2014).
- [21] G. Gao, W. Gao, E. Cannuccia, J. Taha-Tijerina, L. Balicas, A. Mathkar, T. N. Narayanan, Z. Liu, B. K. Gupta, J. Peng, Y. Yin, A. Rubio, and P. M. Ajayan, *Nano Lett.* **12**, 3518 (2014).
- [22] H. Wang, L. Yu, Y.-H. Lee, Y. Shi, A. Hsu, M. L. Chin, L.-J. Li, M. Dubey, J. Kong, and T. Palacios, *Nano Lett.* **12**, 4674 (2012).
- [23] A. Allain, J. Kang, K. Banerjee, and A. Kis, *Nature (London)* **14**, 1195 (2015).
- [24] A. Avsar, I. J. Vera-Marun, J. Y. Tan, K. Watanabe, T. Taniguchi, A. H. Castro Neto, and B. Özyilmaz, *ACS Nano* **9**, 4138 (2015).
- [25] C.-J. Shih, Q. H. Wang, Y. Son, Z. Jin, D. Blankschtein, and M. S. Strano, *ACS Nano* **8**, 5790 (2014).
- [26] T. Roy, M. Tosun, J. S. Kang, A. B. Sachid, S. B. Desai, M. Hettick, C. C. Hu, and A. J. Javey, *ACS Nano* **8**, 6259 (2014).
- [27] L. Yu, Y.-H. Lee, X. Ling, E. J. G. Santos, Y. C. Shin, Y. Lin, M. Dubey, E. Kaxiras, J. Kong, H. Wang, and T. Palacios, *Nano Lett.* **14**, 3055 (2014).
- [28] J. E. Padilha, A. Fazzio, and A. J. R. da Silva, *Phys. Rev. Lett.* **114**, 066803 (2015).
- [29] G. Kresse and J. Furthmüller, *Phys. Rev. B* **54**, 11169 (1996).
- [30] G. Kresse and J. Furthmüller, *Comput. Mater. Sci.* **6**, 15 (1996).
- [31] J. P. Perdew, K. Burke, and M. Ernzerhof, *Phys. Rev. Lett.* **77**, 3865 (1996).
- [32] P. E. Blöchl, *Phys. Rev. B* **50**, 17953 (1994).
- [33] G. Kresse and D. Joubert, *Phys. Rev. B* **59**, 1758 (1999).
- [34] J. Klimes, D. R. Bowler, and A. Michaelides, *J. Phys.: Condens. Matter* **22**, 022201 (2010).
- [35] J. Klimes, D. R. Bowler, and A. Michaelides, *Phys. Rev. B* **83**, 195131 (2011).
- [36] H. Guo, N. Lu, J. Dai, X. Wu, and X. C. Zeng, *J. Phys. Chem. C* **118**, 14051 (2014).
- [37] J. Heyd, G. E. Scuseria, and M. Ernzerhof, *J. Chem. Phys.* **118**, 8207 (2003).
- [38] J. Heyd, G. E. Scuseria, and M. Ernzerhof, *J. Chem. Phys.* **124**, 219906 (2006).
- [39] Within the standard DFT-PBE approach, we find an energy gap of 1.32 eV, and by using the the HSE06 hybrid functional we obtained a band gap of 2.09 eV for a single layer of InSe. In Ref. [40] the authors obtained band gaps of 0.84 eV (PBE) and 1.52 eV (HSE06).
- [40] Y. Cai, G. Zhang, and Y.-W. Zhang, *Sci. Rep.* **4**, 6677 (2014).
- [41] In order to verify the reliability of our results, we check the effect of the (artificial) strain, imposed by the periodic boundary conditions, on the BP and InSe sheets. We calculated the energy positions of the VBM and the CBM of the fully relaxed (unstrained) BP and InSe layers, where we found that the VBM/CBM change by less than 0.02/0.03 eV, thus preserving the type-II band alignment with valence/conduction band offsets of 1.48/0.53 eV.
- [42] G. Graziano, J. Klimes, F. Fernandez-Alonso, and A. Michaelides, *J. Phys.: Condens. Matter* **24**, 424216 (2012).
- [43] R. T. Tung, *Appl. Phys. Rev.* **1**, 011304 (2014).